Scientific Research Publishing

Computational Chemistry, 2018, 6, 27-46
http://www.scirp.org/journal/cc
ISSN Online: 2332-5984
ISSN Print: 2332-5968

Molecular Structure, Electronic Structure, Properties and Analyses of Five Azopyridine Ruthenium Complexes α-Cl, β-Cl, γ-Cl, δ-Cl and ε-Cl of $RuCl_2$(4,6-Dimethyl-Phenylazopyridine)$_2$ as Potential Cancer Drugs: DFT and TD-DFT Investigations

Nobel Kouakou N'Guessan, Kafoumba Bamba*, Ouattara Wawohinlin Patrice, Nahossé Ziao

Laboratoire de Thermodynamique et Physico-Chimie du Milieu, Université Nangui Abrogoua, Abidjan, Côte d'Ivoire
Email: *bambakaf.sfa@univ-na.ci

How to cite this paper: N'Guessan, N.K., Bamba, K., Patrice, O.W. and Ziao, N. (2018) Molecular Structure, Electronic Structure, Properties and Analyses of Five Azopyridine Ruthenium Complexes α-Cl, β-Cl, γ-Cl, δ-Cl and ε-Cl of $RuCl_2$(4,6-Dimethyl-Phenylazopyridine)$_2$ as Potential Cancer Drugs: DFT and TD-DFT Investigations. *Computational Chemistry*, **6**, 27-46.
https://doi.org/10.4236/cc.2018.63003

Received: December 25, 2017
Accepted: July 1, 2018
Published: July 4, 2018

Abstract

Ground state geometries, natural bond orbital (NBO), analysis of frontier molecular orbitals (FMOs), analysis and spectral (RMN and UV-Visible) properties of five azopyridine ruthenium (II) complexes α-Cl, β-Cl, γ-Cl, δ-Cl and ε-Cl of $RuCl_2(Dazpy)_2$ have been theoretically studied by the Density Functional Theory (DFT) and Time-Dependent Density Functional Theory (TD-DFT) methods using two basis sets: Lanl2DZ and a generic basis set in gas or in chloroform solvent. Dazpy stands for 4,6-dimethyl-phenylazopyridine. Optimized geometry shows that, except β-Cl, all the other four isomers α-Cl, γ-Cl, δ-Cl and ε-Cl are C_2 symmetrical. Otherwise, a good agreement was found between experimental and the calculated geometry and NMR data. Moreover, Lanl2DZ effective core potential basis set provides good chemical shifts and geometric properties. Furthermore, the prediction of the frontier orbitals (Highest Occupied Molecular Orbital or HOMO and Lowest Unoccupied Molecular Orbital or LUMO) shows that the most active isomer suitable for electronic reactions is admitted to be δ-Cl. Besides, the NBO analysis indicates that the Ru-N is formed by the electron delocalization of lone pair atomic orbital of N_2 and N_{py} to Ru. Also, the strongest interactions between LP(N) with LP*(Ru) and LP(Cl) with LP*(Ru) stabilize the molecular structure. In addition, NBO shows that the five d orbitals of Ru in the complex are organized so that there is no order of priority from one complex to another. Therefore, the transition LP(Ru) → $\pi^*(N_1 = N_2)$ corresponding to Metal to Li-

gand Charge Transfer (MLCT) is in reality no more than $d \rightarrow \pi^*$. Besides, TDDFT prediction in chloroform solvent reveals that all the five isomerics complexes absorb in the visible region as well as efficient photosensitizers. What's more, δ-$RuCl_2(dazpy)_2$ can potentially act as the excellent sensitizer with a large band of absorption in visible region and a small excited energy. This study can help design and find out the ability or properties of the complex to behave as sensitizer or potential cancer drugs.

Keywords

Azopyridine, DFT, NBO, Pseudo-Potential, Ru(II) Complexes

1. Introduction

Ruthenium (II) azopyridine complexes are attractive because of their electronic, electron-transfer and energy-transfer properties [1] [2]. Azopyridine ligands exhibit both an σ-donor and a π-acceptor character [3] that stabilize ruthenium in the lower oxidation states (II-IV) in complexes [4] [5]. Also, they present a large π-conjugated system that can mediate intermolecular electron or energy transfer process. So, ruthenium (II) complexes with azopyridine ligands are found in wide applications such in electrochemistry and in therapeutic chemistry. In electrochemistry, they have been used as catalyst [6] [7] [8]. In medicinal field, azopyridine compounds, such as the ruthenium (II) with 2-phenylazopyridine (Azpy), $RuCl_2(Azpy)_2$ were discovered to show a remarkable high cytotoxicity against a series of tumour-cell lines [9] [10]. Since their fascinating activity, methylated Azpy derivatives have also been synthesized to improve the previous activities [10] [11]. Therefore, the corresponding ruthenium complexes performed were subsequently tested for their cytotoxicity [10]. Besides, in our previous work, we theoretically investigated the effects of one time methylated Azpy on the electronic structures and related properties [12] [13]. This time, we are interested in studying by quantum methods, ruthenium complexes of twice methylated azopyridine ligand, the 4,6-dimethyl-phenylazopyridine(Dazpy) [14] [15] [16]. The structures of the ligands are shown in **Figure 1**. Thus, the difference between both ligands Dazpy and Azpy comes from two methyl group ($-CH_3$) on the fourth and sixth positions on the pyridine ring. Thanks to literature, these bidentate ligands can bind to ruthenium ion of the reactive $RuCl_3$, $3H_2O$ by the lone electron pairs of their nitrogen atoms N_{py} and N_2, which leads to the formation of a 5-membered stable ring of chelation in the same way as Azpy performs [17]. Therefore, the complexation of ruthenium with an asymmetric ligand actually leads to five different isomerics forms commonly named α-$RuCl_2(Dazpy)_2$ (α-Cl), β-$RuCl_2(Dazpy)_2$ (β-Cl), γ-$RuCl_2(Dazpy)_2$ (γ-Cl), δ-$RuCl_2(Dazpy)_2$ (δ-Cl) and ε-$RuCl_2(Dazpy)_2$ (ε-Cl) as shown in **Figure 2** [18] [19] [20]. Obviously, the difference between the five molecules comes first

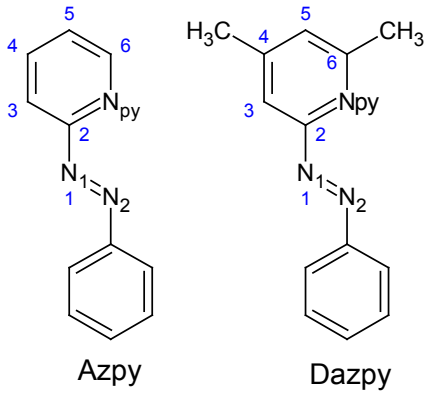

Figure 1. The geometrical structure of 2-phenylazopyridine (Azpy) and 4,6-dimethyl-phenylazopyridine (Dazpy). Dazpy Ligand was obtained from Azpy by substitution of two hydrogen atoms on position 4 and 6 by methyl groups.

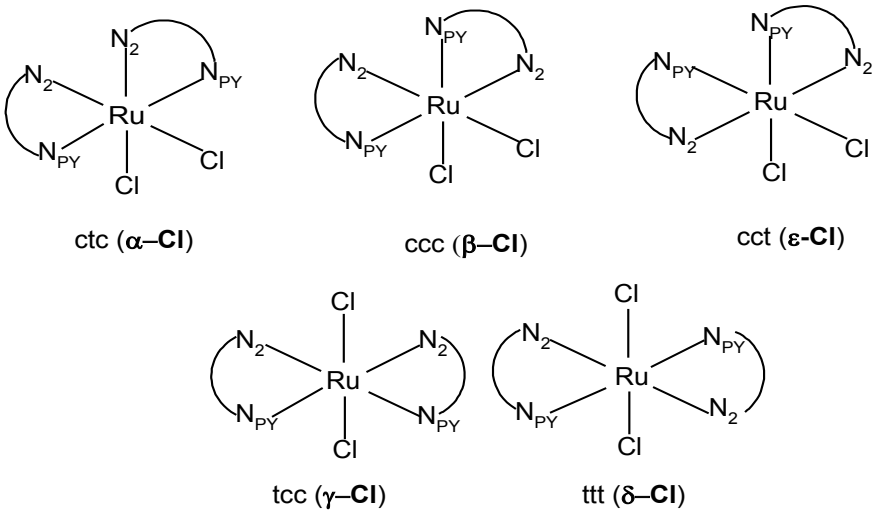

Figure 2. Structures of the five common isomerics azopyridines complexes expected to exist between ruthenium and any azopyridine ligand. Apart from β-Cl, they all present C_2 symmetry. Here, α-Cl, β-Cl and ε-Cl are the *c* is complexes insofar as their both Cl atoms are in *c* is position. Thus, γ-Cl and δ-Cl represent both the *trans* isomers.

from the position of the chloride atoms that divide them up into *cis* or *trans* configurations and secondly from both azopyridine ligands. As yet for $RuCl_2(Dazpy)_2$, only α-Cl displays an experimental data since its structure is confirmed by X-ray crystallography [16].

Currently, the methods of the quantum chemistry are accepted to be indispensable tools to explain or to predict the properties of the compounds [21]. Particularly, the computations that apply the Density Functional Theory (DFT) methods are more reported because of their better consideration of electrons correlation energies and their great reduction of the computation expenses [2] [22] [23]. Therefore, we aim in this work to optimize through DFT investigation, the five α-Cl, β-Cl, γ-Cl, δ-Cl and ε-Cl isomerics of $RuCl_2(Dazpy)_2$ complexes as potential cancer drugs comparatively to $RuCl_2(Azpy)_2$ complexes.

2. Method

All the calculations were performed with DFT method using Becke's three-parameter hybrid B3LYP [24]. The double-zeta pseudo-potential Lanl2DZ [25] basis set is known to be an effective core potential (ECP) which is admitted to display accurate results with transition metals. Besides, it is also suitable for all atom of the periodic table. Before each calculation, the complexes were optimized first with frequency analysis to know of the lack of eventual imaginary vibrational data. This method allows to perform calculations over the most stable molecules in their ground states. All the calculations were performed thanks to Gaussian 03 program package [26]. ^{1}H NMR was calculated at B3LYP/Lanl2DZ. Regarding ruthenium complexes, separate basis set were also considered where ruthenium atom was treated at Lanl2DZ [16] [17] [18] and all the remaining atoms were calculated at B3LYP/6 - 31 g(d). Following the geometric survey, an analysis of the molecular wave function performed in terms of localized electron-pair bonding units using the NBO program is given [27] [28]. This analysis is deemed very important to understand the various interactions involving each component of the complex. In addition, the electronic absorption spectra require calculation of the allowed excitations and oscillator strengths. These calculations were carried out by using TDDFT with the same basis set and exchange-correlation functional in chloroform solution. In addition, the non-equilibrium version of the polarisable continuum model (PCM) [29] [30] was adopted for calculating the solvent effects. Chloroform was chosen as a solvent because the isomer α-$RuCl_2(Dazpy)_2$ was originally synthesized and characterized therein [16]. Hence, TDDFT was used to investigate the absorption properties of all complexes.

3. Results and Discussions

3.1. Molecular Structure

3.1.1. The Geometric Structures

The optimized geometries in vacuum of isomeric complexes of $RuCl_2(Dazpy)_2$ are shown in **Figure 3**. The main computed geometrical parameters e.g. bond lengths and bond angles are listed in **Table 1**. The lone X-ray structure available is that of α-$RuCl_2(Dazpy)_2$. Therefore these experimental data are reported for comparison. Through the optimized geometries, we notice that except β-Cl that presents an lack of symmetry strengthened by the existence of two data per identical bonds, the remaining isomers α-Cl, γ-Cl, δ-Cl and ε-Cl display one data indicating their C_2 symmetry. Anyway, the experimental geometry of α-Cl is reproduced satisfactorily [16]. For instance, the values of bond lengths Ru-N, are comprised between 2.01 and 2.16 Å. These values as well as those of bond angles X-Ru-X (X = Cl or N) are in the same order regarding the comprehensive isomeric $RuCl_2(Azpy)_2$ complexes. This fact provides the DFT to be reliable and the substitution of hydrogen atom by the methyl groups hasn't any real effect on the main bonds lengths or angles of the complexes [12]. Actually, the complex

Table 1. Selected geometrical parameters calculated for isomers *α*-, *β*-, *ε*-, *γ*- and *δ*-$RuCl_2(Dazpy)_2$ at B3LYP/Lanl2DZ and at B3LYP/Gen (Ru = lanl2DZ, C, N and H = 6 - 31 g) levels. Distances are reported in Å and angles in °.

		Ru-N_2	**Ru-N_{py}**	**Ru-Cl_1**	**Ru-Cl_2**	Cl_1-Ru-Cl_2	N_{py}-Ru-N_{py}	N_2-Ru-N_2.
	Lanl.	2.03	2.13	2.51	2.51	95.28	173.05	86.44
***α*-Cl**	gen	2.04	2.15	2.48	2.48	94.84	172.01	86.50
	exp	2.09	2.00	2.41	2.41	82.34	172.41	98.30
***β*-Cl**	Lanl.	2.01 2.03	2.10 2.16	2.50	2.47	89.40	104.66	101.22
	gen	2.03 2.02	2.13 2.19	2.44	2.47	90.23	105.51	101.85
***γ*-Cl**	Lanl.	2.02	2.15	2.49-	2.49-	174.31	105.96	103.10
	gen	2.03	2.18	2.46	2.46	174.07	106.93	104.34
***δ*-Cl**	Lanl.	2.06	2.13	2.49	2.54	180.00	170.49	160.36
	gen	2.07	2.15	2.46	2.51	180.00	171.66	161.78
***ε*-Cl**	Lanl.	2.05	2.12	2.50	2.50	97.91	90.66	176.91
	gen	2.06	2.15	2.46	2.46	97.47	91.75	177.75

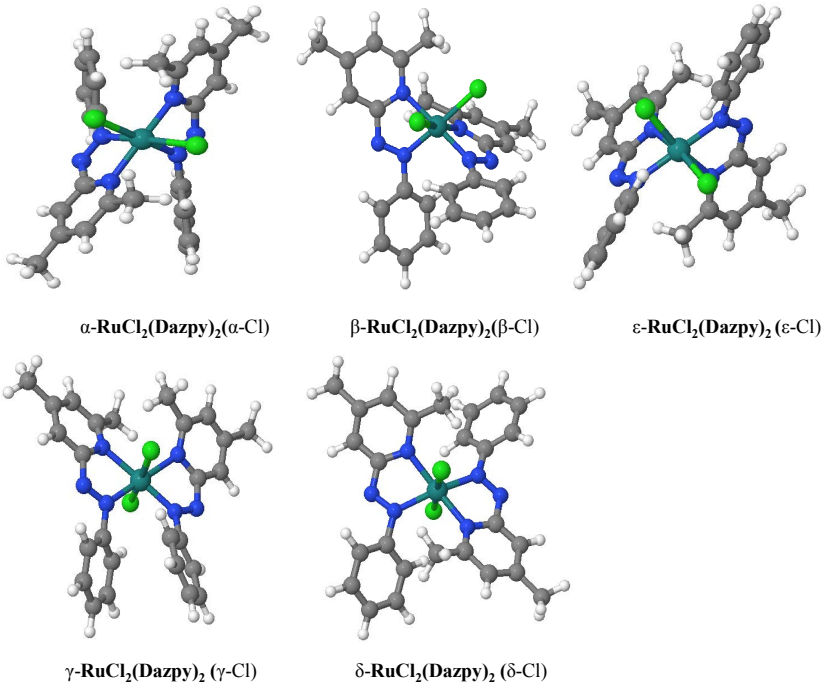

Figure 3. Optimized geometrical structures of isomers *α*-, *β*-, *ε*-, *γ*- and *δ*-$RuCl_2(Dazpy)_2$ at B3LYP/Lanl2DZ level in gas phase. (The green colored sphere corresponds to Ru; the blue colored spheres represent N; the larger dark colored spheres known as C atoms; the smaller white colored spheres stand for H).

$RuCl_2L_2$ displays an octahedral structure. However, the loss of this octahedral shape that doesn't hinder the C_2 symmetry in the case of the $RuCl_2(Azpy)_2$ isomers must be due to Yann Teller's effect [31].

3.1.2. ^{1}H NMR Calculation

All five isomerics azopyridine derivative complexes were theoretically characterized by nuclear magnetic resonance (NMR). In the complexes, only the Dazpy ligand owns all the hydrogen atoms. Therefore, for the purpose of NMR calculation, Figure 4 displays the structure of Dazpy ligand where H is well numbered. Experimentally, all the three protons H_α, as well as the three protons H_γ are identical. Also, the theoretical and experimental chemical shifts of the protons (^{1}H NMR) of all five isomers are resumed in Table 2. The prediction was performed at B3LYP/Lanl2DZ level in vacuum and in chloroform solvent where particularly the PCM method was used for calculation. From Table 2, the gotten theoretically chemical displacements confirm the experimental results in the case of *α*-Cl. The most shielded protons are assumed to be H_α and H_γ of methyl substituent on the pyridine ring. In condensed phases, as well as chloroform solvent, almost the same results are obtained. However, comparatively to gas phase results, they display small chemical shifts.

3.1.3. Natural Bond Orbital (NBO) Analysis

The Natural Bond Orbital (NBO) analysis was developed to study the metal-ligand interactions for all the five isomers $RuCl_2(Dazpy)_2$. This analysis has been performed on the optimized structures of the isomers in gas phase at B3LYP/Lanl2DZ level. The NBO analysis of complexes $RuCl_2(Dazpy)_2$ provides the detailed insight of the nature of electronic conjugation between the bonds within molecule. The natural charges distribution of ruthenium atom, chloride atoms, and ligand Dazpy in complexes are summarized in Table 3. At first glance, we can see a real difference between both groups of isomer regarding the charge of Ru. It is very important in the three *cis* isomers with nearly 0.59 while we have 0.55 in *trans* isomers. Whereas the ligand's charge, it is assumed to be an important factor in the interactions between complexes and the DNA [12] [13] [32]. This importance is rooted in the strength of its bonding by acquiring the electrons from the DNA. Therefore, the ligand that presents the highest charge will develop the best aptitude to bind to the DNA. The natural charge

Table 2. ^{1}H NMR of the five isomers $RuCl_2(Dazpy)_2$ calculated at B3LYP/Lanl2DZ level in gas and in chloroform.

			Gas					Chloroform			Exp
Proton	*α*-Cl	*β*-Cl	*γ*-Cl	*δ*-Cl	*ε*-Cl	*α*-Cl	*β*-Cl	*γ*-Cl	*δ*-Cl	*ε*-Cl	*α*-Cl
H_α	3.77	2.44	2.91	2.34	2.58	3.60	2.47	2.96	2.33	2.59	2.64
H_β	7.68	7.58	7.54	7.48	7.27	8.16	7.95	7.90	7.85	7.64	7.02
H_γ	2.33	2.49	2.51	2.53	2.29	2.56	2.64	2.66	2.66	2.45	2.55
H_δ	7.80	8.38	8.29	8.56	8.16	8.18	8.62	8.51	8.78	8.42	8.22
H_{ortho}	8.20	7.88	8.58	8.72	9.41	8.18	7.91	8.52	8.66	9.38	6.82
H_{meta}	7.54	7.56	7.47	7.85	7.97	7.89	7.78	7.68	8.06	8.16	7.12
H_{para}	7.69	7.75	7.61	8.04	8.09	8.09	8.00	7.85	8.29	8.31	7.30

Table 3. Atomic net charge of Ru, ligand azopyridine and Cl atoms in $|e|$.

Isomers	Ru	Ligand (Q_L)	Cl
α-$RuCl_2(Dazpy)_2$	0.588	0.466	−1.054
β-$RuCl_2(Dazpy)_2$	0.588	0.432	−1.020
γ-$RuCl_2(Dazpy)_2$	0.550	0.486	−1.036
δ-$RuCl_2(Dazpy)_2$	0.551	0.525	−1.076
ε-$RuCl_2(Dazpy)_2$	0.589	0.473	−1.062

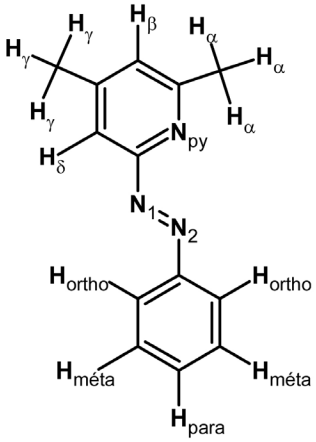

Figure 4. 4,6-dimethyl-[(E)-phenylazo]pyridine (Dazpy) for ^{1}H NMR prediction.

distribution for the five isomers $RuCl_2(Dazpy)_2$ is similar: the positive charges are populated on Ru atoms and the ligand Dazpy. Whereas the negative charge is populated on Cl atoms, since the Cl atoms are the lone responsible for the +II nominal charge of Ru in the complex. Furthermore, the decreasing order of the ligand's charge within the complexes $RuCl_2(Dazpy)_2$ is following: $Q_L(\delta\text{-Cl}) > Q_L(\gamma\text{-Cl}) > Q_L(\varepsilon\text{-Cl}) > Q_L(\alpha\text{-Cl}) > Q_L(\beta\text{-Cl})$. This evolution sequence of the ligand charge Q_L of the isomers is identical to that of the $RuCl_2(Azpy)_2$ isomers [33]. This sequence can be used to predict the order of the affinity link with the DNA as follow: $B(\delta\text{-Cl}) > B(\gamma\text{-Cl}) > B(\varepsilon\text{-Cl}) > B(\alpha\text{-Cl}) > B(\beta\text{-Cl})$. It results from this analysis that the isomer δ-Cl displays the highest value of ligand's charge allowing the strong bonding to DNA. Hens, it is assumed to be the best electron-acceptor ligand. Besides, comparing to the ligand Azpy [33], we notice that Dazpy improves the bonding of all isomers $RuCl_2L_2$ to the DNA by increasing the ligand's charge in the complex.

The natural bond orbital (NBO) method offers supplementary structural information. Table 4 in relation to Table 5 presents the NBOs involved in the metal-ligand interactions for the five isomers $RuCl_2(Dazpy)_2$. Particularly, NBOs presented here regard only Ru-N bondings given that both Ru-Cl bondings are known to be strong Lewis bondings, for they are at the origin of Ru's nominal charge +II [34]. Also, Ru-N bonds are made of the delocalization of electron from a lone pair (LP) orbital of nitrogen atoms towards anti-Lewis lone pairs

Table 4. Occupancy of natural orbitals (NBOs) and hybrids on Cl, N and Ru atoms involved in formation of Ru-Ligand in *α*-, *β*-, *ε*-, *γ*- and *δ*-$RuCl_2(Dazpy)_2$ at B3LYP/Lanl2DZ level.

Donor Lewis-type[a] NBO (Ru-N)	Occupancy	Hybrid[b]	AO(c)[c]	AO(%)[d]
			α-$RuCl_2(Dazpy)_2$	
$LP(N_1)$	1.93	$sp^{1.52}$	$0.63(2s) + 0.46(2p_x) - 0.62(2p_z)$	s(39.64%)p(60.36%)
$LP(N_2)$	1.65	$sp^{1.67}$	$0.61(2s) + 0.45(2p_x) + 0.65(2p_z)$	s(37.43%)p(62.57%)
$LP(N_{py})$	1.68	$sp^{2.69}$	$0.52(2s) + 0.40(2p_x) + 0.74(2p_y)$	s(27.12%)p(72.88%)
LP(Ru)	1.51	$d^{99.99}$	$-0.56(4d_{x^2-y^2}) + 0.83(4d_{z^2})$	p(0.07%)d(99.93%)
LP*(Ru)	0.91	$pd^{99.99}$	$0.98(4d_{xy}) - 0.20(4d_{yz})$	p(0.08%)d(99.92%)
LP*(Ru)	0.81	$sd^{99.99}$	$-0.47(4d_{xy}) + 0.73(4d_{x^2-y^2}) + 48(4d_{z^2})$	s(0.46%)p(0.04%)d(99.49%)
LP*(Ru)	0.27	$sd^{0.01}$	0.995(5s)	s(99.09%)d(0.81%)
			β-$RuCl_2(Dazpy)_2$	
$LP(N_{py})$	1.67	$sp^{2.72}$	$0.52(2s) + 0.22(2p_x) - 0.80(2p_y) - 0.18(2p_z)$	s(26.87%)p(73.13%)
$LP(N_2)$	1.65	$sp^{1.71}$	$0.61(2s) + 0.76(2p_x) - 0.13(2p_y) + 0.18(2p_z)$	s(36.96%)p(63.04%)
$LP(N_1)$	1.93	$sp^{1.58}$	$0.62(2s) - 0.76(2p_x) + 0.14(2p_y) - 0.15(2p_z)$	s(38.71%)p(61.21%)
LP(Ru)	1.65	d^{100}	$0.23(4d_{xz}) + 0.487(4d_{yz}) + 0.36(4d_{x^2-y^2}) + 0.76(4d_{z^2})$	p(0.05%)d(99.95%)
LP*(Ru)	0.93	d^{100}	$0.49(4d_{z^2}) - 0.86(4d_{yz})$	p(0.07%)+d(99.89%)
LP*(Ru)	0.85	d^{100}	$0.13(4d_{yz}) - 0.10(4d_{xz}) - 0.91(4d_{x^2-y^2}) + 0.37(4d_{z^2})$	S(0.09%)p(0.03%)d(99.87%)
LP*(Ru)	0.27	s	0.997(5s)	s(99.44%)d(0.43%)
			γ-$RuCl_2(Dazpy)_2$	
$LP(N_{py})$	1.69	$sp^{2.73}$	$0.52(2s) - 0.70(2p_x) - 0.22(2p_y) - 0.44(2p_z)$	s(26.81%)p(73.19%)
$LP(N_2)$	1.65	$sp^{1.65}$	$0.61(2s) - 0.60(2p_x) - 0.17(2p_y) + 0.49(2p_z)$	s(37.30%)p(62.70%)
$LP(N_1)$	1.93	$sp^{1.52}$	$0.63(2s) - 0.59(2p_x) - 0.19(2p_y) - 0.47(2p_z)$	s(39.74%)p(60.26%)
LP(Ru)	1.62	d^{100}	$0.47(4d_{xy}) + 0.73(4d_{x^2-y^2}) + 0.50(4d_{z^2})$	s(0.03%)d(99.97%)
LP*(Ru)	0.92	$pd^{99.99}$	$0.86(4d_{xy}) - 0.27(d_{x^2-y^2}) - 0.42(4d_{z^2})$	s(0.31%)d(99.97%)
LP*(Ru)	0.83	d^{100}	$0.83(4d_{xz}) - 0.56(4d_{yz})$	d(99.98%)
LP*(Ru)	0.27	$sd^{0.01}$	0.997(5s)	s(99.32%) d(.67%)
			δ-$RuCl_2(Dazpy)_2$	
$LP(N_{py})$	1.68	$sp^{2.66}$	$0.52(2s) + 0.36(2p_x) - 0.77(2p_y)$	s(27.28%)p(72.72%)
$LP(N_2)$	1.68	$sp^{1.62}$	$0.62(2s) + 0.72(2p_x) + 0.30(2p_z)$	s(38.14%)p(61.86%)
$LP(N_1)$	1.93	$sp^{1.53}$	$0.63(2s) - 0.73(2p_x) - 0.27(2p_z)$	s(39.47%)p(60.53%)
LP(Ru)	1.56	d^{100}	$0.46(4d_{xz}) - 0.17(4d_{yz})$	p(0.02%)d(99.98%)
LP*(Ru)	0.9	$sd^{99.99}$	$0.97(4d_{z^2}) - 0.24(4d_{x^2-y^2})$	s(0.3%)d(99.7%)
LP*(Ru)	0.79	d^{100}	$0.23(4d_{z^2}) + 0.32(4d_{xy}) + 0.92(4d_{x^2-y^2})$	s(0.26%)p(0.01%)d(99.73%)
LP*(Ru)	0.26	$sd^{0.01}$	0.995(5s)	s(99.05%)d(0.92%)
			ε-$RuCl_2(Dazpy)_2$	
$LP(N_{py})$	1.67	$sp^{2.62}$	$0.52(2s) - 0.51(2p_x) + 0.25(2p_y) + 0.63\ (2p_z)$	s(27.62%)p(72.38%)
$LP(N_2)$	1.68	$sp^{1.70}$	$0.61(2s) + 0.65(2p_x) + 0.44(2p_y)$	s(37.10%)p(62.90%)
$LP(N_1)$	1.93	$sp^{1.53}$	$0.63(2s) - 0.63(2p_x) - 0.44(2p_y)$	s(39.58%)p(60.42%)
LP(Ru)	1.62	d^{100}	$0.38(4d_{z^2}) - 0.82(4d_{xy}) - 0.41(4d_{x^2-y^2})$	s(0.09%)p(0.01%)d(99.90%)
LP*(Ru)	0.87	$pd^{99.99}$	$0.49(4d_{z^2}) - 0.19(4d_{x^2-y^2}) - 0.85(4d_{xy})$	p(0.02%)p(99.90%)
LP*(Ru)	0.84	$d^{99.99}$	$0.99(4d_{yz}) + 0.13(4d_{xz})$	p(0.01%)p(99.99%)
LP*(Ru)	0.27	s	0.998(5s)	s(99.68%)d(0.23%)

Table 5. Second-order interaction energy (E_2. kcal/mol) between donor and acceptor orbitals in $RuCl_2L_2$ complexes at B3LYP/Lanl2DZ level. The three LP*(Ru) are numbered here 4, 5 and 6 to highlight their difference. In reference to **Table 4**, the numbers are indicated in respect to decreasing occupancy.

Donor →acceptor	E_2	E(j)-E(i)	F(i.j)	Donor → acceptor	E_2	E(j)-E(i)	F(i.j)
	α-$RuCl_2(Dazpy)_2$				β-$RuCl_2(Dazpy)_2$		
$LP(N_2) \rightarrow LP_4^*(Ru)$	74.29	0.28	0.153	$LP(N_2) \rightarrow LP_4^*(Ru)$	95.57	0.28	0.172
$LP(N_2) \rightarrow LP_5^*(Ru)$	31.62	0.31	0.101	$LP(N_2) \rightarrow LP_5^*(Ru)$	16.01	0.3	0.071
$LP(N_2) \rightarrow LP_6^*(Ru)$	21.07	0.67	0.109	$LP(N_2) \rightarrow LP_6^*\_Ru$	25.08	0.7	0.121
$LP(N_{py}) \rightarrow LP_5^*(Ru)$	77.03	0.24	0.138	$LP(N_{py}) \rightarrow LP_4^*\_Ru$	50.36	0.21	0.11
$LP(N_{py}) \rightarrow LP_6^*(Ru)$	25.54	0.6	0.112	$LP(N_{py}) \rightarrow LP_5^*(Ru)$	42.94	0.23	0.103
$LP(Ru) \rightarrow \pi^*(N_1\text{-}N_2)$	20.12	0.13	0.046	$LP(N_{py}) \rightarrow LP_6^*(Ru)$	21.38	0.63	0.105
$LP(Cl) \rightarrow LP_4^*(Ru)$	89.59	0.08	0.091	$LP_3\_Ru \rightarrow \pi^*(N_1\text{-}N_2)$	16.68	0.14	0.046
$LP(Cl) \rightarrow LP_5^*(Ru)$	34.97	0.11	0.064	$LP(Cl) \rightarrow LP_4^*(Ru)$	127.55	0.08	0.105
$LP(Cl) \rightarrow LP_6^*(Ru)$	34.34	0.48	0.117	$LP(Cl) \rightarrow LP_5^*(Ru)$	18.31	0.1	0.105
				$LP(Cl) \rightarrow LP_6^*(Ru)$	35.31	0.5	0.122
	γ-$RuCl_2(Dazpy)_2$				δ-$RuCl_2(Dazpy)_2$		
$LP(N_2) \rightarrow LP_4^*(Ru)$	82.43	0.28	0.157	$LP(N_2) \rightarrow LP_5^*(Ru)$	53.91	0.3	0.130
$LP(N_2) \rightarrow LP_5^*(Ru)$	18.52	0.28	0.077	$LP(N_2) \rightarrow LP_4^*(Ru)$	29.67	0.29	0.099
$LP(N_2) \rightarrow LP_6^*(Ru)$	29.61	0.69	0.130	$LP(N_2) \rightarrow LP_6^*(Ru)$	25.89	0.68	0.12
$LP(N_{py}) \rightarrow LP_5^*(Ru)$	65.86	0.21	0.123	$LP(N_{py}) \rightarrow LP_5^*(Ru)$	73.17	0.24	0.134
$LP(N_{py}) \rightarrow LP_4^*(Ru)$	14.74	0.21	0.060	$LP(N_{py}) \rightarrow LP_4^*(Ru)$	3.41	0.22	0.029
$LP(N_{py}) \rightarrow LP_6^*(Ru)$	23.49	0.62	0.108	$LP(N_{py}) \rightarrow LP_5^*(Ru)$	25.75	0.61	0.113
$LP(Ru) \rightarrow \pi^*(N_1\text{-}N_2)$	12.77	0.14	0.038	$LP_3\_Ru \rightarrow \pi^*(N_1\text{-}N_2)$	18.28	0.14	0.045
$LP(Cl) \rightarrow LP_4^*(Ru)$	112.88	0.11	0.117	$LP(Cl) \rightarrow LP_4^*(Ru)$	104.08	0.11	0.108
$LP(Cl) \rightarrow LP_6^*(Ru)$	25.61	0.51	0.106	$LP(Cl) \rightarrow LP_5^*(Ru)$	10.75	0.12	0.036
				$LP(Cl) \rightarrow LP_4^*(Ru)$	24.46	0.5	0.102
	ε-$RuCl_2(Dazpy)_2$						
$LP(N_2) \rightarrow LP_4^*(Ru)$	94.60	0.29	0.172	$LP(Ru) \rightarrow \pi^*(N_1\text{-}N_2)$	12.83	0.14	0.038
$LP(N_2) \rightarrow LP_6^*(Ru)$	26.79	0.68	0.122	$LP(Cl) \rightarrow LP_4^*(Ru)$	33.12	0.10	0.059
$LP(N_{py}) \rightarrow LP_4^*(Ru)$	24.68	0.23	0.078	$LP(Cl) \rightarrow LP_5^*(Ru)$	81.32	0.10	0.094
$LP(N_{py}) \rightarrow LP_5^*(Ru)$	64.71	0.23	0.127	$LP(Cl) \rightarrow LP_6^*(Ru)$	33.01	0.50	0.118
$LP(N_{py}) \rightarrow LP_6^*(Ru)$	19.58	0.62	0.10				

orbital LP* of Ru. Indeed, the LP orbitals of the nitrogen atoms which population are far less than 2 electrons are those actually involved in the formation of Ru-N bondings. For instance, N_1 cannot link to Ru in so far that $LP(N_1)$ owns 1.93e that approximates 2e occupancies in all complexes. Thus, both N_2 and N_{py} are only the involved atoms regardless the nature of the isomer. This result highlights the bidentate state and the σ-donor character of azopyridine ligand. Furthermore, ruthenium atom owns six NBOs made of three donors (LP) and three

acceptors (LP*). These orbitals are also made of linear combination of the six valence orbitals known as $4d_{xy}4d_{xz}4d_{yz}4d_{x^2-y^2}4d_{z^2}5s$ which are common to all metallic atoms of the fifth row of the periodic table and whereupon only the difference stems in the allotment of their valence electrons. Table 6 shows the electronic structure of the valence orbital of ruthenium when it is alone or within the complex. It discloses that there is no degeneration of atomic orbitals for they present different energy and electrons are shared differently over them. Apart from γ-$RuCl_2(Dazpy)_2$, δ-$RuCl_2(Dazpy)_2$ and $RuCl_3{,}3H_2O$ where t_{2g} (d_{xy}, d_{xz}, d_{yz}) and e_g($d_{x^2-y^2}$, d_{z^2}) orbitals are slightly ordered, the *cis* isomers don't respect any order. Thus, the five atomic orbitals of Ru are disorganized. It means that both the presence of the Dazpy ligand and the nature of the isomer whatsoever modify Ru's electronic structure. Otherwise, the five orbitals that are supposed to be degenerated in metal, cease to have the same energy in presence of ligand and there is no rule indicating the most stable of them from one isomer to another as conventionally stated in literature. Anyhow, this changing of the state of Ru's structure that doesn't affect the symmetry of the isomer can be attributed to the Yahn Teller effect [31].

Regarding the five isomers in Table 4, only four of LP and LP* NBOs of Ru whose populations of electrons are comprised between 1.57 and 0.27 are involved in the octahedral Ru-Ligand formation. The three LP*NBO of the ruthenium are the lone acceptors from the ligand with which Ru binds and the LP is the electron donor. This latest orbital is assumed to be the responsible for the MLCT transition. For more understanding, the meaningful donor-acceptor interactions between NBOs in complexes investigated by second order perturbation

Table 6. Electronic structure of the valence orbital and their energy for the five isomers of $RuCl_2(Dazpy)_2$ complexes, the reactive $RuCl_3{,}3H_2O$ and Ru atom.

Complexes		Structure electronic of Ru						valence electrons
α-$RuCl_2(Dazpy)_2$	Structure	$(4d_{yz})^{1.89}$	$(4d_{xy})^{1.68}$	$(4d_{z^2})^{1.37}$	$(4d_{xz})^{0.95}$	$(4d_{x^2-y^2})^{1.19}$	$(5s)^{0.27}$	7.35
	Energy	−0.221	−0.215	−0.202	−0.199	−0.187	0.208	
β-$RuCl_2(Dazpy)_2$	Structure	$(4d_{xy})^{1.94}$	$(4d_{xz})^{1.70}$	$(4d_{z^2})^{1.36}$	$(4d_{yz})^{1.09}$	$(4d_{x^2-y^2})^{0.99}$	$(5s)^{0.28}$	7.36
	Energy	−0.237	−0.224	−0.212	−0.204	−0.186	0.231	
γ-$RuCl_2(Dazpy)_2$	Structure	$(4d_{x^2-y^2})^{1.67}$	$(4d_{z^2})^{1.69}$	$(4d_{yz})^{1.50}$	$(4d_{xy})^{1.09}$	$(4d_{xz})^{1.14}$	$(5s)^{0.28}$	7.37
	Energy	−0.227	−0.212	−0.206	−0.199	−0.188	0.237	
δ-$RuCl_2(Dazpy)_2$	Structure	$(4d_{yz})^{1.93}$	$(4d_{xy})^{1.81}$	$(4d_{xz})^{1.57}$	$(4d_{z^2})^{0.89}$	$(4d_{x^2-y^2})^{0.91}$	$(5s)^{0.27}$	7.38
	Energy	−0.222	−0.217	−0.215	−0.181	−0.170	0.217	
ε-$RuCl_2(Dazpy)_2$	Structure	$(4d_{x^2-y^2})^{1.67}$	$(4d_{xz})^{1.38}$	$(4d_{z^2})^{1.63}$	$(4d_{xy})^{1.10}$	$(4d_{yz})^{1.31}$	$(5s)^{0.27}$	7.36
	Energy	−0.222	−0.213	−0.212	−0.193	−0.192	0.221	
$RuCl_3.3H_2O$	Structure	$(4d_{xy})^{1.99}$	$(4d_{yz})^{1.99}$	$(4d_{xz})^{1.21}$	$(4d_{z^2})^{0.83}$	$(4d_{x^2-y^2})^{0.76}$	$(5s)^{0.28}$	7.06
	Energy	−0.290	−0.288	−0.263	−0.249	−0.232	0.235	
Ru atom	Structure	$(4d_{xy})^2$	$(4d_{xz})^2$	$(4d_{yz})^2$	$(4d_{z^2})^{1.51}$	$(5s)^{0.49}$	$(4d_{x^2-y^2})^0$	8
	Energy	−0.200	−0.181	−0.180	−0.148	−0.119	−0.100	

theory are listed in Table 5. The perturbation donor-acceptor analysis of the NBO method offers the information about intermolecular interactions. The highest values of the calculated energies point out the strongest interactions between LP(N) with LP*(Ru) and LP(Cl) with LP*(Ru) that stabilize the molecular structure. Besides, the high value of LP(N) → LP*(Ru) interaction emphasizes the σ-donation of the ligand Dazpy. We can also notice in Table 5 that the three LP*(Ru) are involved almost together in the same interaction with whatever ligand through a sort of linear combination so that the perturbation energy from both LP(N_{py}) and LP(N_2) to LP*(Ru) are identical confirming the bidentate state of the ligand Dazpy. Concerning the LP(Ru) → $\pi^*(N_1\text{-}N_2)$ interaction, the less value recorded comparing with LP(N) → LP*(Ru) shows the small retro-donation but more significant. The ruthenium lone pair donor LP(Ru) is composed of the orbital d of ruthenium while the $\pi^*(N_1\text{-}N_2)$ are formed by p orbital of the nitrogen atoms within the ligand. Here, the interaction LP(Ru) → $\pi^*(N_1\text{-}N_2)$ indicates the electron delocalization regarding the metal to ligand charge transfer (MLCT). Owing to the particularity of Dazpy ligand to mix the five atomic d orbitals, the transition therefore is assumed to be d → π^*.

3.2. Frontier Molecular Orbital Energies

The Frontier Molecular Orbitals (FMOs), in particular Highest Occupied Molecular Orbital (HOMO) and Lowest Unoccupied Molecular Orbital (LUMO) play an important role in spectra and chemical reactions, as they govern many chemical reactions [35]. The HOMO and LUMO orbitals distributions computed at B3LYP/Lanl2DZ level for the isomerics complexes of $RuCl_2(Dazpy)_2$ are illustrated in Figure 5. In addition, the compositions of the FMOs have been calculated and presented in Table 7. It shows that the component of HOMO of the five complexes is concentrated on the ruthenium atom and comes mainly from d

Table 7. Frontier molecular orbital HOMO (H) and LUMO (L) and the compositions of the ground states of *α*-, *β*-, *γ*-, *δ*- and *ε*-$RuCl_2(Dazpy)_2$, at the B3LYP/Lanl2DZ in gas.

Isomers	Molecular Orbital		Energy (eV)	Composition (%)			Main Bond type
	index	orbital		Ru	Cl	Ligand	
***α*-Cl**	128	L	−3.297	1	2	97	d(Ru) + p(Cl) + π(dazpy)
	127	H	−5.278	50	28	22	d(Ru) + p(Cl) + π(dazpy)
***β*-Cl**	128	L	−3.011	14	2	84	d(Ru) + p(Cl) + π(dazpy)
	127	H	−5.406	45	31	24	d(Ru) + p(Cl) + π(dazpy)
***γ*-Cl**	128	L	−3.098	8	3	89	d(Ru) + p(Cl) + π(dazpy)
	127	H	−5.293	55	24	21	d(Ru) + p(Cl) + π(dazpy)
***δ*-Cl**	128	L	−3.234	2	3	96	d(Ru) + p(Cl) + π(dazpy)
	127	H	−5.162	62	24	13	d(Ru) + p(Cl) + π(dazpy)
***ε*-Cl**	128	L	−3.244	6	2	92	d(Ru) + p(Cl) + π(dazpy)
	127	H	−5.178	57	30	13	d(Ru) + p(Cl) + π(dazpy)

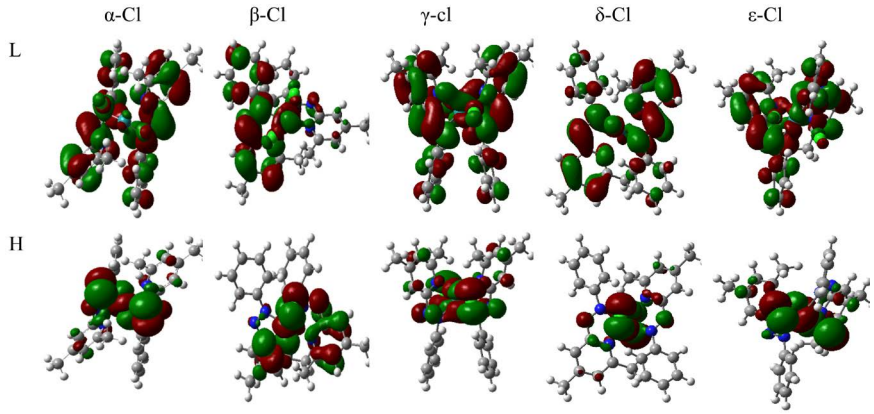

Figure 5. Frontier molecular orbitals and associated electronic transitions for $RuCl_2(Dazpy)_2$ calculated at B3LYP/LanL2DZ in Gas phase.

orbitals of the metal. So, it may be characterized by d orbitals of the ruthenium. Whereas for the LUMO, it comes mainly from p orbitals of C and N atoms of the ligands. As result, the electronic transitions between both orbitals are assigned to singlet metal-to-ligand charge-transfer transitions (^{1}MLCT) [36]. Thus, their spectral characteristics are similar to that of the well known complex $RuCl_2(Azpy)_2$ [12].

Since then, the HOMO-LUMO energy separation ΔE has been used as simple indicator of kinetic stability and chemical reactivity. The reactivity of the complexes is closely related to the energy gap between the HOMO and the LUMO of the compounds [37] [38]. Then, the narrower the ΔE, the higher will be the reactivity and the lower will then be the kinetic stability. Otherwise, a small value of the gap indicates a great reactivity and a low kinetic stability. In reference to that, the growing order of reactivity is β-Cl < γ-Cl < α-Cl < ε-Cl < δ-Cl. This evolution sequence of reactivity shows that δ-$RuCl_2(Dazpy)_2$ isomer is the most reactive while β-$RuCl_2(Dazpy)_2$ exhibits the highest kinetic stability. Besides, comparing both ligands, we notice that Dazpy improves the reactivity of the isomers α-Cl and ε-Cl. Nevertheless, regarding the complexes reactivities, the most reactive remains δ-$RuCl_2(Azpy)_2$ [33].

The energy values of the highest occupied molecular orbital (HOMO) and the lowest unoccupied molecular orbital (LUMO), the gap energy between HOMO and LUMO, the chemical potential and hardness were determined at the same level and summarized in **Table 8**. The energy of LUMO plays an important role in the process of binding the complex to DNA. Indeed, a low LUMO energy of the complex promotes the intercalation [39] [40]. Because the low LUMO energy of the complex easily accepts electrons from the HOMO of the DNA base pairs. Besides, **Table 8** makes it possible to establish the decreasing order of the energy of the LUMO as α-Cl < ε-Cl < δ-Cl < γ-Cl < β-Cl. This order indicates the α-Cl isomer, because of the small value of its LUMO as the best candidate to bind to the DNA. Again, comparing both ligands Azpy and Dazpy [33], we notice that all isomers of Dazpy reduce the affinity of bonding to the DNA insofar

Table 8. Frontier orbital energies and relatives characterizing the reactivity of azopyridine ruthenium complexes in eV calculated at B3LYP/LANL2DZ level.

	α-Cl	*β*-Cl	*γ*-Cl	*δ*-Cl	*ε*-Cl
HOMO	−5.278	−5.406	−5.293	−5.162	−5.178
LUMO	−3.297	−3.011	−3.098	−3.243	−3.244
*Δ*E	1.981	2.395	2.195	1.919	1.934
μ	−4.288	−4.209	−4.196	−4.203	−4.211
η	0.990	1.198	1.098	0.960	0.967

as they increase the value of the energy of their LUMO orbital.

Moreover, the ability of a compound to accept electrons from an electron donor is indicated by the chemical potential *μ*. So, the comparison of the chemical potential of the five $RuCl_2(Dazpy)_2$ isomers shows that *α*-$RuCl_2(Dazpy)_2$ isomer is more electron acceptor since its chemical potential is the lowest. Furthermore, the electron transfer ability can also be approximated by the chemical hardness. Also, the analysis of the hardness values shows that the *α*-Cl isomer is the softest compound because of its low chemical hardness and the *β*-Cl isomer is assumed to be the hardest isomer. Therefore, we can conclude that the double methylation on pyridine rings increases the hardness.

The solubility of a compound is a determining criterion as for their efficiency and their utility in the pharmacopeia. The solubility of the compounds in aqueous solution can also be valued by the determination of the sharing coefficient log P. This size can be approximated by using the dipole moment. Indeed, the dipole moment indicates the stability of a molecule in water. So, a strong dipole moment will trigger a weak solubility in the organic solvents and a strong solubility in water [33]. **Table 9** presents the computed dipole moment of the five isomers $RuCl_2(Dazpy)_2$. So, the decreasing order of the dipole moment is: $\mu(\varepsilon\text{-Cl}) > \mu(\beta\text{-Cl}) > \mu(\alpha\text{-Cl}) > \mu(\gamma\text{-Cl}) > \mu(\delta\text{-Cl})$. This trend of the dipole moment value reveals that the isomer *δ*-Cl is the most soluble compound in the organic solvents while the isomer *ε*-Cl represents the most soluble in aqueous solution. Consequently, the *δ*-Cl isomer shall display the highest cytotoxicity. Furthermore, the double methyl group on pyridine of Azpy ligand decreases the dipole moment in all isomers comparatively to the reference $RuCl_2(Azpy)_2$ [12] [33] [41].

3.3. Electronic Absorption Spectra

In order to explore the electron transition between the energy levels, the lowest singlet → singlet spin allowed excited states are to be considered. With the optimized ground state geometries as the starting point, TD-DFT method at B3LYP/Lanl2DZ level with PCM in chloroform solvent was developed to calculate absorption spectra of the five isomerics complexes. This method can help find out the ability for the complex to behave as sensitizer [42]. To understand

Table 9. Dipole moment of the five isomers α-, β-, ε-, γ- et δ-$RuCl_2(Dazpy)_2$ calculated in Debye.

	μ			
isomers	μ_x	μ_y	μ_z	μ_{total}
α-$RuCl_2(Dazpy)_2$	0	0	−7.9187	7.9187
β-$RuCl_2(Dazpy)_2$	1.6237	3.4162	8.2658	9.0901
γ-$RuCl_2(Dazpy)_2$	0	0	3.1755	3.1755
δ-$RuCl_2(Dazpy)_2$	0	0	1.4287	1.4287
ε-$RuCl_2(Dazpy)_2$	0	0	−10.5219	10.5219

the transition behavior, the maximum absorption wavelengths (λ_{max}), excitation energies (ΔE), the oscillator strengths (f), the frontier orbital's composition and the main transitions regarding the visible region are summarized in **Table 10**. The simulated UV-visible spectrum of the comprehensive complexes of $RuCl_2(Dazpy)_2$ in chloroform is shown in **Figure 6**. Therein, all five isomeric complexes absorb in the visible region (400 - 800 nm) thereby stressing their efficient photosensitivity [43]. The general UV-visible spectra of $RuCl_2(Dazpy)_2$ complexes described (**Figure 6**) exhibits two different bands of absorption. The first band that is absorbed in UV region is attributed to ligand to ligand charge transfer LLCT $\pi \rightarrow \pi^*$. This transition is centered mainly on azopyridine ligand and the regarding wavelength for all complexes is lower than 500 nm. The second band localized in the visible region at $\lambda > 500$ nm is attributed to metal to ligand charge transfer transition (MLCT) d → π^*, with d sub-shell belonging Ru atom as abovementioned and π^* corresponds to orbital p from the ligand (**Table 7**). In fact, the HOMO of $RuCl_2(Dazpy)_2$ complexes is essentially made of metal atomic orbitals. Regarding the LUMO orbital, it is exclusively made of azopyridine atomic orbitals for all the studied complexes, which is consistent with MLCT transition. The theoretical absorption spectrums of α-Cl, β-Cl, ε-Cl, γ-Cl and δ-Cl isomers of $RuCl_2(Dazpy)_2$ present the MLCT transitions respectively, at 669.14 nm (f = 0.094), 587.495 nm (f = 0.143), 615.615 nm (f = 0.073), 567.878 nm (f = 0.216) and 722.944 nm (f = 0.139). In the case of α-Cl and δ-Cl, the electron leaves from HOMO-1 orbital to LUMO orbital, while for β-Cl and ε-Cl isomers, the MLCT corresponds to the transition from HOMO-2 orbital to LUMO+1 orbital. Concerning the γ-Cl isomer, the MLCT transition corresponds to the departure of electron from HOMO to LUMO+1. Furthermore, **Table 10** lists the calculated excited state lifetimes of all five $RuCl_2(Dazpy)_2$ isomers. The excited state life time is one of the most important parameters to study the efficiency or the charge transfer [44], for it tends to maintain for long time the dyes in the cationic state that is more favorable to the charge transfer [44] [45] [46]. In reality, the excited state lifetime of the dye can be evaluated via the following equation: $\tau = 1.499/f\sigma^2$, where τ is the excited wave number of the different electronic states (cm^{-1}) and f is the oscillator strength corresponding to

Table 10. Absorption properties of isomers *α*-Cl, *β*-Cl, *ε*-Cl, *γ*-Cl and *δ*-Cl isomers of $RuCl_2(Dazpy)_2$ comprising the excited energy, the maximum wavelength, oscillation frequency f, the main transitions involved by the energy and the excited state lifetime.

Isomers	composition of frontierorbitals		ΔE(eV)	λ_{max}(nm)	*f*	Main transition	*τ*(ns)
	HOMO	LUMO					
α-Cl	Ru (57%)	Dazpy (96%)	1.853	669.140	0.094	H-1 → L (55%)	71.39
			2.771	447.659	0.058	H-3 → L+1 (56%)	51.74
			3.079	402.718	0.153	H-8 → L (56%)	15.89
β-Cl	Ru (55%)	Dazpy (85%)	2.110	587.495	0.143	H-2 → L+1 (44%)	36.19
			2.817	440.068	0.080	H-4 → L+1 (53%)	36.30
			3.174	388.460	0.064	H-6 → L+1 (38%)	35.74
γ-Cl	Ru (52%)	Dazpy (90%)	2.183	567.878	0.216	H → L+1 (57%)	22.39
			2.700	459.135	0.285	H-3 → L+1 (69%)	11.09
			3.362	368.783	0.151	H-4 → L+1 (44%)	13.50
δ-Cl	Ru (67%)	Dazpy (96%)	1.715	722.944	0.139	H-1 → L (69%)	56.36
			2.953	419.889	0.262	H-6 → L (50%)	10.09
ε-Cl	Ru (63%)	Dazpy (92%)	2.014	615.615	0.073	H-2 → L+1 (58%)	77.82
			2.643	469.142	0.110	H-3 → L (65%)	29.99
			2.941	421.560	0.238	H-6 → L (64%)	11.19

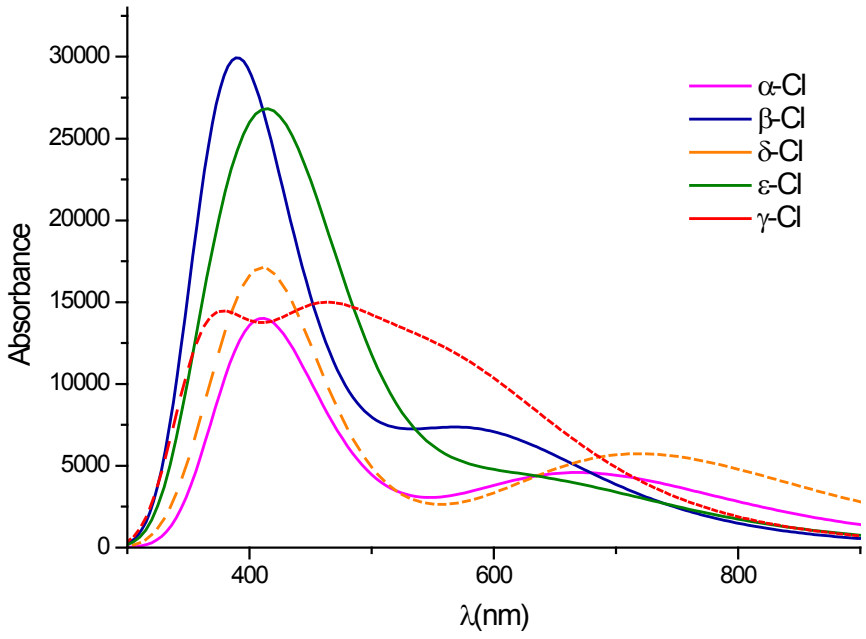

Figure 6. Simulated absorption spectra of both isomers *α*-Cl, *β*-Cl, *ε*-Cl, *γ*-Cl and *δ*-Cl of $RuCl_2(Dazpy)_2$, from TD-DFT calculations at the B3LYP/Lanl2DZ level in chloroform.

the electronic state. Therefore, it turns out from Table 10 that *ε*-Cl shows the highest excited state value. However, as *Δ*E indicates the energy required to excite the complex, *δ*-Cl is assumed to be the best sensitizer since it not merely displays the widest wavelengths (λ_{max} = 722.9 nm) but also shows a relatively

important excited state lifetime $56.36.10^{-9}$ns.

4. Conclusion

In the present work, we have performed theoretical investigations on the properties of ruthenium complexes $RuCl_2(Dazpy)_2$ in ground and excited state. The geometry optimization, IR, NMR and UV-visible spectra properties, natural bond orbital (NBO) analysis and frontier molecular orbital analysis of five isomeric complexes of $RuCl_2(Dazpy)_2$ were investigated by using DFT and TD-DFT methods at B3LYP level. The pseudopotential Lanl2DZ basis and generic basis were used to perform the calculation. Afterwards B3LYP/Lanl2DZ was chosen for all remaining calculations. The calculated geometry and NMR data were compared with the experimental values of α-$RuCl_2(Dazpy)_2$ and a good agreement was found. Besides, the NBO analysis indicates that the Ru-N are dative bonds and are formed by the electron delocalization of lone pair atomic orbital of N_2 and N_{py} to the three anti lone pairs orbitals of Ru. Also, the strongest interactions between LP(N) with LP*(Ru) and LP(Cl) with LP*(Ru) stabilize the molecular structure. In addition, NBO also shows that the five d orbitals degenerated in metal alone are completely separated, since they have different energy in the complex. Moreover, we found out that there is no priority order when sharing electrons between the five d orbitals. This must certainly be due to the ligand Dazpy. Therefore, owing to the mixing of these d orbitals, the transition LP(Ru) → $\pi^*(N_1\text{-}N_2)$ corresponding to MLCT is assumed to be $d \rightarrow \pi^*$ confirming the ability for the azopyridine ruthenium complexes to be used as photo sensitizer. Furthermore, the δ-$RuCl_2(Dazpy)_2$ isomer with small gap energy is admitted to be the best reactive and most cytotoxic ruthenium complex. Regarding TDDFT prediction, it also reveals that δ-$RuCl_2(Dazpy)_2$ is admitted to be an excellent sensitizer because of a large band of its absorption spectra in the visible region and its small excited energy ΔE.

References

[1] Heeres, A., van Doren, H., Gotlieb, K. and Bleeker, I. (1997) Synthesis of α- and β-d-Glucopyranuronate 1-Phosphate and α-d-Glucopyranuronate 1-Fluoride: Intermediates in the Synthesis of d-Glucuronic Acid from Starch. *Carbohydrate Research,* **299**, 221-227. https://doi.org/10.1016/S0008-6215(97)00030-X

[2] Ziegler, M. and Zelewsky, A.V. (1998) Charge-Transfer Excited State Properties of Chiral Transition Metal Coordination Compounds Studied by Chiroptical Spectroscopy. *Coordination Chemistry Reviews,* **177**, 257-300. https://doi.org/10.1016/S0010-8545(98)00186-6

[3] Dougan, S.J., Melchart, M., Habtemariam, A., Parsons, S. and Sadler, P.J. (2006) Phenylazo-Pyridine and Phenylazo-Pyrazole Chlorido Ruthenium (II) Arene Complexes: Arene Loss, Aquation and Cancer Cell Cytotoxicity. *Inorganic Chemistry*, **45**, 10882-10894. https://doi.org/10.1021/ic061460h

[4] Basuli, F., Das, A., Mostafa, G., Peng, S.M. and Bhattacharya, S. (2000) Chemistry of Ruthenium with Some Phenolic. *Polyhedron*, **19**, 1663-1672. https://doi.org/10.1016/S0277-5387(00)00404-6

[5] Boelrijk, A.E.M., Anja, M., Jorna, J. and Reedijk, J. (1995) Containing a 2-(Phenyl) Azopyridine or a 2-(Nitrophenyl)Azopyridine Ligand. *Journal of Molecular Catalysis A*: *Chemical*, **103**, 73-85. https://doi.org/10.1016/1381-1169(95)00112-3

[6] Barf, G.A. and Sheldon, R.A. (1995) Ruthenium (II) 2-(Phenylazo) Pyridine Complexes as Epoxidation Catalysts. *Journal of Molecular Catalyst A*: *Chemiccoll*, **98**, 143-146. https://doi.org/10.1016/1381-1169(95)00026-7

[7] Bamba, K. (2004) Oxydation électrocatalytique de monosaccharides sur des complexes de ruthénium et sur le platine modifié par des adatomes métalliques. PhD Thesis, University of Poitiers, Poitiers, 70.

[8] Bamba, K., Leger, J.M., Garnier, E., Bachmann, C., Servat, K. and Kokoh, K.B. (2005) Selective Electro-Oxidation of D-Glucose by RuCl2(azpy)2 Complexes as Electrochemical Mediators. *Electrochimica Acta*, **50**, 3341-3346. https://doi.org/10.1016/j.electacta.2004.12.007

[9] Velders, A.H., Kooijman, H., Spek, A.L., Haasnoot, J.G., De Vos, D. and Reedijk, J. (2000) Strong Differences in the *in Vitro* Cytotoxicity of Three Isomeric Dichlorobis(2-Phenylazopyridine)Ruthenium(II) Complexes. *Inorganic Chemistry*, **39**, 2966-2967. https://doi.org/10.1021/ic000167t

[10] Hotze, A.C.G., Caspers, S.E., de Vos, D., Kooijman, H.S.A.L., Flamigni, A., Marina, B., Sava, G., Haasnoot, J.G. and Reedijk, J. (2004) Structure-Dependent *in Vitro* Cytotoxicity of the Isomeric Complexes [RuL2Cl2] (L = o-Tolylazopyridine and 4-Methyl-2-Phenylazopyridine) in Comparaison to [Ru(azpy)2Cl2]. *Journal of Biological Inorganic Chemistry*, **9**, 354-364. https://doi.org/10.1007/s00775-004-0531-6

[11] Changsaluk, U. and Hansongnern, K. (2005) Dichlorobi(5methyl-2-(phenylazo) pyridine) Ruthénium (II) Complex: Charaterisation and NMR Sepectroscopy. *Songklanakarin Journal of Science and Technology*, **27**, 739-749.

[12] N'Guessan, K.N., Kafoumba, B., Ouattara, W.P. and Nahossé, Z. (2017) Theoretical Investigation of the Structure Activity Relationships (SARs) of a Series of Five Isomeric α, β, γ, δ, ε Ruthenium Complexes RuCl2L2 with Azopyridine Ligands [L = azpy, tazpy, 4mazpy, 5mazpy]. *International Journal of Engineering Research and Application*, **7**, 58-70. https://doi.org/10.9790/9622-0706015870

[13] Kouakou, N.N., Mamadou, R.K., Kafoumba, B., Ouattara, W.P. and Nahossé, Z. (2017) Quantitative Structure Anti-Cancer Activity Relationship (QSAR) of a Series of Ruthenium Complex Azopyridine by the Density Functional Theory (DFT) Method. *Computational Molecular Bioscience*, **7**, 19-31. https://doi.org/10.4236/cmb.2017.72002

[14] Ackermann, M.N., Moore, K.B., Colligan, A.S., Thomas-Wohlever, J.A. and Warren, K.J. (2003) Inorganic Chemistry in Nuclear Imaging and Radiotherapy: Current and Future Directions. *Journal of Organometallic Chemistry*, **667**, 81-89. https://doi.org/10.1016/S0022-328X(02)02140-X

[15] Ackermann, M.N., Fairbrother, W.G., Amin, N.S., Deodene, C.J., Lamborg, C.M. and Martin, P.T. (1996) Tetracarbonylmolybdenum Complexes of 2-(phenylazo)pyridine Ligands. Correlations of Molybdenum-95 Chemical Shifts with Electronic, Infrared, and Electrochemical Properties. *Journal of Organometallic Chemistry*, **523**, 145-151.

[16] Kooijman, H., Hotze, C.G., Capers, S.E., Haasnoot, J.G., Reedijk, J. and Spek, A.L. (2004) α-Dichlorobis(2-phenylazo-4,6-dimathylpyridine)ruthénium (II) Chloroform. *Acta Crystallographica E*, **60**, m247-m249. https://doi.org/10.1107/S1600536804001618

[17] Affi, S.T., Bamba, K. and Ziao, N. (2015) Computational Characterization of Organometallic Ligands Coordinating Metal: Case of Azopyridine Ligands. *Journal of Theoretical and Computational Chemistry*, **14**, Article ID: 1550006. https://doi.org/10.1142/S0219633615500066

[18] Goswami, S., Chakravarty, A.R. and Chakravorty, A. (1981) Chemistry of Ruthenium. 2. Synthesis, Structure, and Redox Properties of 2-(arylazo)pyridine Complexes. *Inorganic Chemistry*, **20**, 2246-2250. https://doi.org/10.1021/ic50221a061

[19] Bao, T., Krause, K. and Krause, R.A. (1988) Hydroxide-Assisted Stereospecific Isomerization of a Trans-Dichlorobischelate of Ruthenium (II). *Inorganic Chemistry*, **27**, 759-761. https://doi.org/10.1021/ic00277a037

[20] Velders, A.H., van der Schilden, K., Hotze, A.A., Reedijk, J., Kooijman, H. and Spek, A.L. (2004) Dichlorobis(2-phenylazopyri dine)ruthenium(II) Complexes: Characterisation, Spectroscopic and Structural Properties of Four Isomers. *Dalton Transactions*, 448-455. https://doi.org/10.1039/B313182C

[21] Jäger, M., Freitag, L. and González, L. (2015) Using Computational Chemistry to Design Ru Photosensitizers with Directional Charge Transfer. *Coordination Chemistry Reviews*, **304-305**, 146-165. https://doi.org/10.1016/j.ccr.2015.03.019

[22] Petersson, G.A., Malick, D.K., Wilson, W.G., Ochterski, J.W., Montgomery, J.A. and Frisch, J.M.J. (1998) Calibration and Comparison of the Gaussian-2, Complete Basis Set, and Density Functional Methods for Computational Thermochemistry. *The Journal of Chemical Physics*, **109**, Article ID: 10570. https://doi.org/10.1063/1.477794

[23] Zheng, K.C., Kuang, D.B., Wang, J.P. and Shen, Y. (2000) Electronic Structure and Related Chemical Properties of Complexes $M(bpy)^{2+}_3$(M=Fe,Ru,Os). *Acta Physico-Chimica Sinica*, **16**, 608. https://doi.org/10.3866/PKU.WHXB20000707

[24] Becke, A.D. (1993) A New Mixing of Hartree-Fock and Local Density-Functional Theories. *The Journal of Chemical Physics*, **98**, 1372-1377. https://doi.org/10.1063/1.464304

[25] Foresman, J.B. and Frisch, E. (1996) Exploring Chemistry with Electronic Structure Methods. Second Edition, Gaussian Inc., Pittsburgh.

[26] Frisch, M., Trucks, G., Schlegel, H., Scuseria, G., Robb, M., Cheeseman, J., Montgomery, J.J., Vreven, T., Kudin, K., Burant, J., Millam, J., Iyengar, S., Tomasi, J., Barone, V., Mennucci, B., Cossi, M., Scalmani, G., Rega, N., Petersson, H., Nakatsuji, M., Hada, M., Ehara, K., Hasegawa, J., Fukuda, R., Toyota, K., Ishida, M., Nakajima, T., Honda, Y., Kitao, O., Nakai, H., Klene, M., Li, X., Knox, J.E., Hratchian, H.P., Cross, J.B., Bakken, V., Adamo, C., Jaramillo, J., Gomperts, R., Stratmann, R.E., Yazyev, O., Austin, J.A., Cammi, R., Pomelli, C., Ochterski, J.W., Ayala, P.Y., Morokuma, K., Voth, G.A., Salvador, P., Dannenberg, J.J., Zakrzewski, V.G., Dapprich, S., Daniels, A.D., Strain, M.C., Farkas, O., Malick, K., Rabuck, D., Raghavachari, K., Foresman, J.B., Ortiz, J.V., Cui, Q., Baboul, A.G., Clifford, S., Cioslowski, J., Stefanov, B.B., Liu, G., Liashenko, A., Piskorz, P., Komaromi, I., Martin, R.L., Fox, D.J., Keith, T., Al-Laham, M.A., Peng, Y.C., Nanayakkara, A., Challacombe, M., Gill, P.W., Johnson, B., Chen, W., Wong, M.W., Gonzaler, C. and Pople, J.A. (2004) Gaussian 03, Revision E.01. Gaussian, Wallingford.

[27] Reed, A.E., Curtiss, L.A. and Weinhold, F. (1988) Intermolecular Interactions from a Natural Bond Orbital, Donor-Acceptor Viewpoint. *Chemical Review*, **88**, 899-926.

[28] Glendening, E.D., Reed, A.E., Carpenter, J.E. and Weinhold, F. (1996-2001) The NBO3.0 Program. University of Wisconsin, Madison.

[29] Barone, V. and Cossi, M. (1998) Quantum Calculation of Molecular Energies and Energy Gradients in Solution by a Conductor Solvent Model. *The Journal of Physical Chemistry A*, **102**, 1995-2001. https://doi.org/10.1021/jp9716997

[30] Cossi, M., Rega, N., Scalmani, G. and Barone, V. (2003) Energies, Structures, and Electronic Properties of Molecules in Solution with the C-PCM Solvation Model. *Journal of Computational Chemistry*, **24**, 669-681. https://doi.org/10.1002/jcc.10189

[31] Shriver, D.F. and Atkins, P. (1999) Inorganic Chemistry. 3rd Edition, Oxford University Press, New York, 235-236.

[32] Chen, J.C.L.J., Qian, L. and Zheng, K.C. (2005) Electronic Structures and SARs of the Isomeric Complexes α-, β-, γ-[Ru(mazpy)2Cl2] with Different Antitumor Activities. *Journal of Molecular Structure*: *THEOCHEM*, **728**, 93-101. https://doi.org/10.1016/j.theochem.2005.05.005

[33] Bamba, K., Patrice, O., Nobel, N. and Ziao, N. (2016) SARs Investigation of α-, β-, γ-, δ-, ε-RuCl2(Azpy)2 Complexes as Antitumor Drugs. *Computational Chemistry*, **4**, 1-10. https://doi.org/10.4236/cc.2016.41001

[34] Oziminski, W., Narbutt, J., Michalik, J. and Smułek, W. (2010) Theoretical Investigations on the Structure Bonding in Neutral Trinitrate Complexes of Americium (III) and Europium (III) with. Centre of Radiochemistry and Nuclear Chemistry.

[35] Singh, R.K., Verma, S.K. and Sharma, P.D. (2011) DFT Based Study of Interaction between Frontier Orbitals of Transition Metal Halides and Thioamides. *International Journal of Chemtech Research*, **3**, 1571-1579.

[36] Juris, A., Balzani, V., Barigelletti, F., Campagna, S., Belser, P. and von Zelewsky, A. (1988) Ru(II) Polypyridine Complexes: Photophysics, Photochemistry, Eletrochemistry, and Chemiluminescence. *Coordination Chemistry Reviews*, **84**, 85-277. https://doi.org/10.1016/0010-8545(88)80032-8

[37] Vitnik, V.D., Vitnik, Z.J., Banjac, N.R., Valentic, N.V., Uscumlic, G.S. and Juranic, I.O. (2014) Quantum Mechanical and Spectroscopic (FT-IR, 13C, 1H NMR and UV) Investigations of Potent AntiepilepticDrug 1-(4-Chloro-Phenyl)-3-Phenyl Succinimide. *Spectrochimica Acta Part A*: *Molecular and Biomolecular Spectroscopy*, **117**, 42-53. https://doi.org/10.1016/j.saa.2013.07.099

[38] Prasad, M., Sri, N., Veeraiah, A., Veeraiah, V. and Chaitanya, K. (2013) Molecular Structure, Vibrational Spectroscopic (FT-IR, FT-Raman), UV-Vis Spectra, First Order Hyperpolarizability NBO Analysis, HOMO and LUMO Analysis, Thermodynamic Properties of 2,6-Dichloropyrazine by *Ab Inito* HF and Density Functional Method. *Journal of Atomic and Molecular Sciences*, **4**, 1-17.

[39] Fleming, I. (1976) Frontier Orbitals and Organic Chemical Reactions. John Wiley & Sons, New York.

[40] Chen, L., Liu, L., Chen, J.C., Shi, S., Tan, C.T., Zheng, K.C. and Ji, L.N. (2008) Experimental and Theoretical Studies on the DNA-Binding and Spectral Properties of Water-Soluble Complex $[Ru(MeIm)4(dpq)]^{2+}$. *Journal of Molecular Structure*, **881**, 156-166. https://doi.org/10.1016/j.molstruc.2007.09.010

[41] Chen, J.C., Li, J., Wu, W. and Zheng, K.C. (2006) Structures and Activities of a Series of the Isomeric Complexes $RuCl_2(azpy)_2$. *Acta Physico-Chimica Sinica*, **22**, 391-396.

[42] Fan, W.J., Cai, J.W., Yang, G.J., Chi, J.W., Zhou, D., Tan, D.Z. and Zhang, R.Q. (2016) Aggregation of Metal-Free Organic Sensitizers on TiO_2(101) Surface for Use in Dye-Sensitized Solar Cells: A Computational Investment. *Computational and Theoretical Chemistry*, **1093**, 1-8. https://doi.org/10.1016/j.comptc.2016.08.006

[43] Umer, M., Ibnelwaleed, A.H., Muhammad, D., Shakeel, A. and Khalil, H. (2015)

Theoretical Study of Benzene/Thiophene Based Photosensitizers for Dye Sensitized Solar Cells (DSSCs). *Dyes and Pigments*, **118**, 152-158. https://doi.org/10.1016/j.dyepig.2015.03.003

[44] Shalabi, A., El Mahdy, A., Taha, H. and Soliman, K. (2005) The Effects of Macrocycle and Anchoring Group Replacements on the Performance of Porphyrin Based Sensitizer: DFT and TD-DFT Study. *Journal of Physics and Chemistry of Solids*, **76**, 22-33. https://doi.org/10.1016/j.jpcs.2014.08.002

[45] Li, M., Kou, L., Diao, L., Zhang, Q., Li, Z., Wu, Q., Lu, W., Pan, D. and Wei, Z. (2015) Theoretical Study of WS-9-Based Organic Sensitizers for Unusual vis/NIR Absorption and Highly Efficient Dye-Sensitized Solar Cells. *Journal of Physics and Chemistry of Solids*, **119**, 9782-9790.

[46] Sun, C., Li, Y., Song, P. and Ma, F. (2016) An Experimental and Theoretical Investigation of the Electronic Structures and Photoelectrical Properties of Ethyl Red and Carminic Acid for DSSC Application. *Materials*, **9**, E813. https://doi.org/10.3390/ma9100813